Increased core ion temperatures in high-beta advanced scenarios in ASDEX Upgrade

M. Reisner[1,2], E. Fable[1], J. Stober[1], A. Bock[1], A. Bañon Navarro[1], A. Di Siena[1], R. Fischer[1], V. Bobkov[1], R. McDermott[1], and the ASDEX Upgrade Team[3]

[1]Max-Planck-Institut für Plasmaphysik, 85748 Garching bei München, Germany
[2]Ludwig-Maximilian-Universität, München, Germany
[3]See the author list of H. Meyer et al. 2019 Nucl. Fusion 59 112014

April 6, 2020

Abstract

Non-inductive advanced Tokamak scenarios are a possible way for future nuclear fusion power plants to run in non-pulsed operation. In these scenarios, the ohmic current is replaced on the one hand with a current driven by external sources such as NBI and ECRH and on the other hand with a substantial bootstrap-current. The bootstrap current is produced in the presence of pressure gradients. This means, to increase the bootstrap-current-fraction, it is advantageous to have regions where ITG turbulence is reduced. To be able to extrapolate from non-inductive scenarios done in smaller present day devices, it is important to have transport models that allow the user to reproduce these experiments and accurately capture the physics behind the reduction of turbulent transport. One commonly used model is the quasi-linear gyrofluid transport model TGLF, which is well tested in standard scenarios. However, in the past, TGLF has failed to reproduce the peaked ion temperature profiles of certain advanced scenario shots.

In this article, progress in overcoming this issue of TGLF will be discussed. Results of a recent publication are reproduced in which TGLF was able to match the experimentally measured peaked ion temperature profiles. In these simulations, we find the E×B-shear to play an important role in the reduction of ITG turbulence. In contrast to that, experimentally we find the E×B-shear to have no effect on the formation of such regions of decreased turbulent transport. This finding is in line with simulations using the gyrokinetic code GENE. A new approach of modelling these advanced scenarios in TGLF is introduced, allowing us to match the peaked ion temperature profiles without depending on the E×B-shear.

1 Introduction

One drawback of conventional Tokamak scenarios is that they need to be run in pulsed operation. To make future fusion power plants based on the Tokamak design economically more viable, they require non-inductive operation or at least an increased pulse length. Such non-inductive or long-pulse scenarios are called Advanced Tokamak scenarios. In these advanced scenarios, the inductively driven current is replaced with a current driven by external sources like NBI and ECRH on the one hand, and with a substantial bootstrap-current on the other hand. External current sources require to spend additional energy, which reduces the effective energy-output of the fusion device. It is therefore desirable to maximise the contribution of the bootstrap-current to the total plasma-current. Since the bootstrap-current is created in the presence of pressure gradients, internal transport barriers (ITBs) or regions of decreased turbulent transport are favourable to such scenarios, as the achievable pressure gradients in tokamaks are generally limited by turbulent transport. In particular, ion heat transport is thought to be dominated by the ion temperature gradient (ITG) driven mode, which means that processes that locally increase the stability of ITG modes are favourable in advanced scenarios.

One example for such a nearly non-inductive high beta discharge with a region of reduced turbulent transport is the ASDEX Upgrade (AUG) discharge #32305 with an H_{89}(y,2) greater than one and $\beta_{\mathrm{N}} = 2.7$ [1]. In this nearly non-inductive discharge, between 40 and 50 % of the current is made up by the bootstrap current, supported by the peaked temperature profiles that come with the reduced turbulent transport.

To be able to extrapolate from such experiments done in the smaller present-day devices, it is important to have transport models that are able to reproduce these experiments. One such commonly used transport model is the quasilinear TGLF [2] (Trapped Gyro Landau Fluid), which is based on runs of the gyrokinetic code GYRO and works well in standard scenarios [3][4][5][6]. As shown in [7] and [8], however, TGLF has problems reproducing the peaked ion temperature profiles often observed in such high-beta non-inductive advanced scenarios.

In references [7], [9] and [10], using the gyrokinetic code GENE [11], it was found that fast ions play an important role in the reduction of the turbulent transport. The main process is that they act as a catalyst for the transfer of energy from the ITG to subdominant modes, reducing the ITG drive, which results in less transport. This nonlinear electromagnetic fast ion effect, however, is not yet implemented in TGLF. In TGLF, including fast ions has only a stabilising effect by diluting the main ions and by affecting the equilibrium. In [7], a comparison between TGLF and GENE also showed a non-negligible difference in simulations without fast ions, which indicates that on top of the fast ion effect, also the contribution of the thermal pressure is not captured entirely correct in TGLF.

In this article, possible ways to implement all the relevant physics required to stabilise ITG turbulence in TGLF are investigated and compared against

experimental results.

In section 2 we discuss recent advances in modelling such regions of decreased transport using TGLF and will show that the E×B-shear plays a central role in these simulations. Because of conflicting results coming from GENE that suggest a much smaller contribution of the E×B-shear, experiments have been done with the aim to investigate the contribution of the E×B-shear to the formation of regions of reduced turbulent transport. The results of these experiments, conducted in AUG, will be shown in section 3. In this section, we furthermore show the results of TGLF simulations of these new AUG discharges, using the same setup as the simulations done in section 2. Since the results of the simulations in section 3 are not a very good match, in section 4 we introduce a new approach to modelling these regions of decreased transport and show first preliminary results of this new method. Finally, in section 5 we then sum up our findings and give an outlook to the work yet to be done.

2 Simulations

While gyrokinetic codes like GENE are powerful tools that allow the user to make accurate predictions and help understand the relevant physics needed to correctly describe certain scenarios, their runs are very expensive both in time and computing resources. Therefore, to explore different scenario designs, it is important to have transport codes that can simulate entire profiles in a shorter range of time. This requires the programs to be based on reduced physics models. One such reduced model is the quasilinear transport model TGLF, which combines its linear set of equations with so-called saturation rules that determine when and how turbulence goes into saturation. These rules were calibrated on a substantial number of runs of the gyrokinetic code GYRO. Where nonlinear local simulations of gyrokinetic codes like GYRO or GENE can take several days until they are finished, simulations of TGLF are done in seconds – of course at the expense of physics fidelity. Used inside a framework transport code, TGLF can also be used to simulate entire profiles. The simulations conducted over the course of this study use TGLF inside the transport code ASTRA [12][13].

In standard scenarios, such as the ones it was benchmarked against, TGLF is able to accurately reproduce the experimental results. However, in non-standard scenarios, this is not always the case, as was for instance reported in reference [1], where TGLF was not able to recover the peaked ion temperature profiles of the high-beta non-inductive AUG discharge #32305. Despite that, in a recent publication [14], TGYRO/TGLF simulations of the same discharge are reported to be in good agreement with the experimental measurements. There are several reasons contributing to this differing result:

First, in the simulations in [14], fast ions were included, in contrast to [1], where they were not included, neither in the pressure nor as a kinetic species. Secondly, in [14] a newer version of TGLF was used, in which the so-called quench-rule, which handles the suppression of turbulence by the E×B-shear, was replaced by the so-called spectral-shift-model [15].

Additional differences include that in [1] only T_i was allowed to evolve while T_e was kept fixed, whereas in [14] both temperature profiles were allowed to evolve. Furthermore, in ASTRA the equilibrium is recalculated in each time step, while in TGYRO it is kept fixed over the whole simulation. Finally, due to a misinterpretation of experimental data, the rotation profile used in [1] was lower than the experimentally measured one, though this alone is not sufficient to explain the difference.

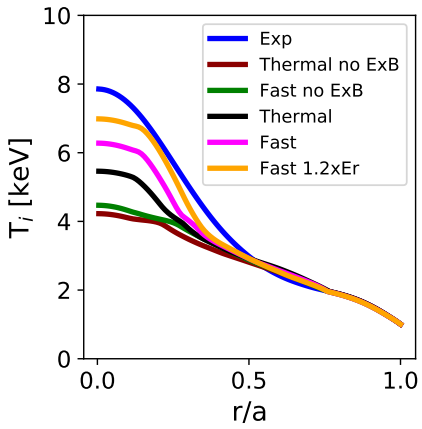

Figure 1: Ion temperature profiles resulting from TGLF simulations of the AUG shot #32305 between 3.5-4.0 s, compared to the experimentally measured profile. Simulations labelled "fast" include fast ions as a kinetic species and the contribution of fast ions to the total pressure. Simulations labelled "thermal" only include thermal ions. Simulations labelled "no E×B" have the radial electric fields set to 0 and therefore do not include E×B-shear effects, simulations without this label include E×B effects. The simulation labelled "Fast 1.2xEr" include fast ions combined with an increased E×B-shear.

When these differences are taken into account, it is in fact possible to recover the profiles also using ASTRA/TGLF (see Fig. 1).

In these simulations, TGLF-Sat0 using the spectral-shift E×B-rule was used inside the transport code ASTRA. To keep the equilibrium fixed, like in the TGYRO/TGLF-simulations, the regular temperature variables in ASTRA, TE and TI representing the electron and ion temperature respectively, were set constant, and instead additional auxiliary variables F_1 and F_2 were used to calculate the evolution of the temperature profiles. While F_1 and F_2 were used as the temperatures that went as input into the TGLF calculations, the fixed TE and TI still went into the calculation of the equilibrium. This way, it was possible to keep the equilibrium fixed.

The input power going into the simulation was calculated by TORBEAM in the case of ECRH and by TRANSP/NUBEAM in the case of NBI. Radiation losses were tomographically reconstructed from bolometric measure-

ments. As boundary condition for the temperatures, the experimental profiles at $\rho_{\mathrm{tor}} = 0.75$ were used, averaged over a time interval between 3.5 and 4.0 seconds. In Fig. 1, the results of different TGLF simulations are shown, using both fast ion and E×B-effects, only one of each or neither. It can be seen that in the case without E×B effects, both the simulation using only thermal ions and the simulation using additionally fast ions can not recover the peaked ion temperature profiles.

If E×B effects are taken into account, then both the thermal and the fast ion simulations result in a peaked profile, though in the fast ion case it is much more pronounced. Finally, it was found that the simulations are very sensitive toward the precise value of the E×B-shear. Changing the radial electric field and therefore also the E×B-shear by about 20 % has a significant effect on the resulting $\mathrm{T_i}$-profile. A change of this magnitude is still justified, as the poloidal rotation that goes into the values of $\mathrm{E_r}$ used in this publication comes from neoclassical calculations. Taking the poloidal rotation instead from measurements leads to the radial electric field increasing by 20 %, in the case of this discharge.

In Fig. 2a, the results of a series of TGLF standalone simulations are shown, in which the E×B-shear is varied, further illustrating the strong dependence of the ion heat flux on $\omega_{E\times B}$ in TGLF, at the operational point this experiment is located.

Contrary to that, in figure 2b a similar scan is shown, resulting from a series of GENE simulations. There, the strong dependency of the ion heat flux on the E×B-shear is not observed.

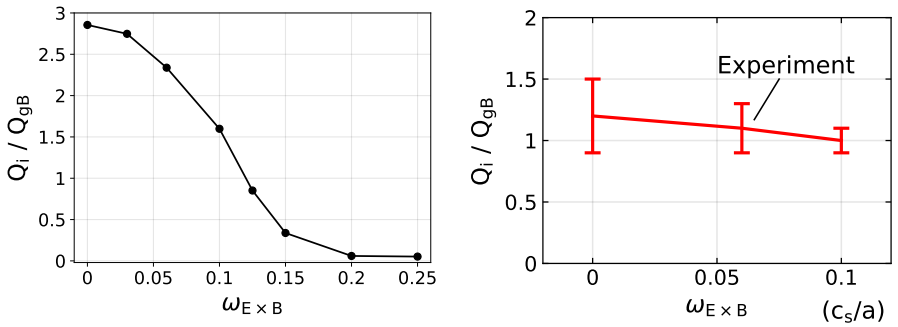

(a) (b)

Figure 2: Dependence of the ion heat flux on the E×B-shear using TGLF standalone simulations (a) and nonlinear GENE simulations (b). In TGLF varying around the experimentally found E×B-shear of $\omega_{\mathrm{E\times B}} = 0.06$ (indicated in (b)) strongly changes $\mathrm{Q_i}$, whereas in GENE there is only a much smaller effect.

While it is safe to assume that GENE is describing the situation more accurately, the assumption that the E×B-shear plays an important role in the formation of internal transport barriers is at least plausible, as it is also gener-

ally accepted to be the main cause of the formation of the edge transport barrier in the plasma edge. To test the strength of the effect of the E×B-shear, an experiment has been conducted that will be described in the following section.

3 Experiments

In this section, an experiment conducted in the tokamak ASDEX Upgrade is described, which investigates the effect of the E×B-shear on the ion temperature gradient. Time-traces of this plasma-discharge can be seen in Fig. 3.

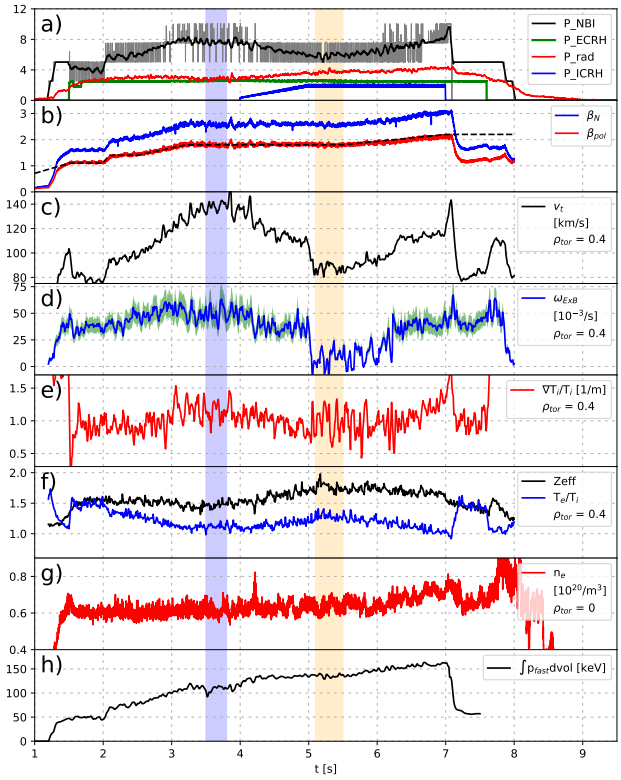

Figure 3: Time evolution of the AUG shot #35938. In box (a) one can see the heating mix, in box (b) the plasma beta. In box (c) the toroidal rotation is shown, in box (d) the E×B-shear resulting from it can be seen. In box (e) the logarithmic ion temperature gradient is displayed. Box (f) contains the effective charge Z_{eff} and the temperature ratio T_e/T_i while in box (g) the electron density n_e is shown. In box (h) the integrated fast ion pressure is displayed. Shaded in blue and orange, respectively, are two flattop phases, with and without ICRF-heating, that are examined in more detail in this article.

This discharge #35938 is based on the discharge #32305 investigated in the previous section. Like #32305, it has a toroidal magnetic field of 2.5 T on axis and a plasma-current of 800 kA. After an initial ohmic ramp-up of the current, approximately 2.5 MW of ECRH are added and NBI is slowly ramped up by the β-feedback-control to values of 8 to 10 MW, matching β_{pol} to a pre-programmed curve (dashed line in Fig. 3c) that stays constant at $\beta_{\mathrm{pol}} = 1.8$ for the main part of this discharge. Under these heating conditions, T_{i} becomes slightly peaked. After a flattop-phase, approximately 2.5 MW of ICRF are slowly added, causing the beta-feedback-control to reduce NBI. Reducing the number of energetic particles injected with a parallel component into the plasma then leads to a reduced torque which significantly reduces the toroidal rotation $\mathrm{v_t}$. According to equation 1

$$\omega_{E\times B} = \frac{\varepsilon}{q}\frac{\partial}{\partial\rho_{\mathrm{tor}}}\frac{E_{\mathrm{r}}}{B_{\mathrm{p}}} = \frac{\varepsilon}{q}\frac{\partial}{\partial\rho_{\mathrm{tor}}}\frac{v_{\mathrm{t}}\cdot B_{\mathrm{p}} - v_{\mathrm{p}}\cdot B_{\mathrm{t}} + \frac{\nabla p_{\mathrm{imp}}}{Z_{\mathrm{imp}}\cdot e\cdot n_{\mathrm{imp}}}}{B_p} \tag{1}$$

this then leads to a reduction of the E×B-shear.

Here, E_{r} is the radial electric field, v_{t} and v_{p} are the toroidal and poloidal rotation velocity of boron, B_{t} and B_{p} are the toroidal and poloidal magnetic field and Z_{imp} and n_{imp} are the charge and density of the boron impurity. $p_{\mathrm{imp}} = n_{\mathrm{imp}} \cdot T_{\mathrm{imp}}$ is the impurity pressure and finally e the elementary charge. As its contribution to the overall $\mathrm{E_r}$ is very small, the diamagnetic term $\frac{1}{B_{\mathrm{p}}}\frac{\nabla p_{\mathrm{imp}}}{Z_{\mathrm{imp}}\cdot e\cdot n_{\mathrm{imp}}}$ is neglected.

The components of the magnetic fields are determined with the equilibrium reconstruction code IDE[16]; v_{t} and $\mathrm{T_i}$ are measured using CXRS, and a fit through the data was done using the Gaussian process regression code IDI[17]. For v_{p} neoclassical values calculated with the transport code TRANSP were used. These values for v_{p} are in agreement with the values of $v_{\mathrm{p}} = 0 \pm 2\,km/s$ obtained by comparing the difference between v_{t} obtained from CXRS at the high- and low-field-side of the plasma.

Between the first and second flattop phase indicated in Fig. 3, a strong decrease in v_{t} was achieved, resulting in a significant change in $\omega_{\mathrm{E\times B}}$. Between those two time intervals, only a very small decrease in $\nabla T_{\mathrm{i}}/T_{\mathrm{i}}$ is observed – if any. This can also be seen very well in the radial profiles depicted in Fig. 4. There the blue curves are an average over the first flattop-phase indicated in Fig. 3, with only NBI and EC heating, the orange curves are an average over the second flattop-phase, during which additional ICRF heating was applied. The red line indicates the radial position $\rho_{\mathrm{tor}} = 0.4$, the position the time-trace in Fig. 3 was taken from.

In the left part of Fig. 4, the radial profiles of $\omega_{\mathrm{E\times B}}$ can be seen. In the interval between $\rho_{\mathrm{tor}} = 0.3$ and $\rho_{\mathrm{tor}} = 0.5$, a clear reduction can be observed by a factor of approximately 6, going from $\omega_{\mathrm{E\times B}} \approx 60 \cdot 10^3/\mathrm{s}$ to $\omega_{\mathrm{E\times B}} \approx 10 \cdot 10^3/\mathrm{s}$. When comparing the ion temperature gradient between the two time intervals, there is essentially no change in $\nabla T_{\mathrm{i}}/T_{\mathrm{i}}$.

Looking at the time-trace of the logarithmic ion temperature gradient, a small, gradual decrease between the two time-intervals can be seen. Since both

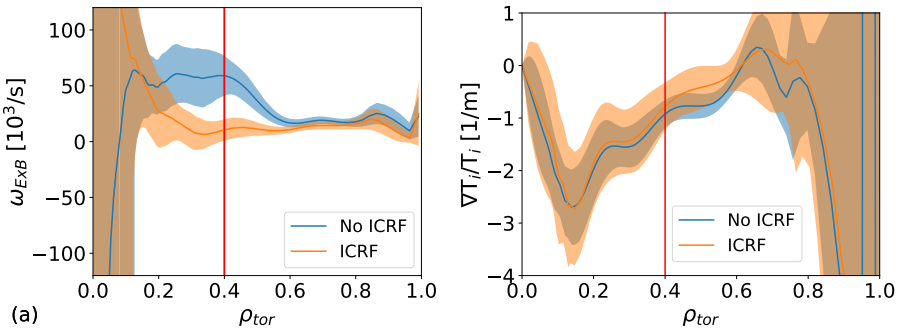

Figure 4: Radial profiles of the E×B-shear (a) and the logarithmic ion temperature gradient (b). Blue lines correspond to an average over the first time interval indicated in Fig. 3, orange lines to the average over the second one. The shaded regions represent the sum of one standard deviation of that average and the propagated measurement uncertainties. The red lines indicate the radial position $\rho_{\mathrm{tor}} = 0.4$, at which position the time-traces in Fig. 3 were plotted.

$\mathrm{v_t}$ and $\omega_{\mathrm{E\times B}}$ have a discrete drop around 5 s, corresponding to the end of the ICRF-ramp, it stands to reason that this change in E×B-shear is not the cause for the decrease in $\nabla T_\mathrm{i}/T_\mathrm{i}$. Instead, this minute decrease can be attributed to the increase in $T_\mathrm{e}/T_\mathrm{i}$ stemming from the change in the heating scheme we have done.

Throughout the discharge, n_e does not change. According to

$$n_\mathrm{i} = n_\mathrm{e} \cdot \left(1 - \frac{Z_\mathrm{eff} - 1}{Z_\mathrm{imp}}\right), \tag{2}$$

$\mathrm{n_i}$ decreases, because $\mathrm{Z_{eff}}$ increases slightly while ICRF is used. The logarithmic gradients of both $\mathrm{n_e}$ and $\mathrm{n_i}$, however, do not change between the two time intervals. This, together with the almost negligible decrease in $\nabla T_\mathrm{i}/T_\mathrm{i}$, leads us to the conclusion that there is no significant effect of the ExB-shear on ITG turbulence in the core region. In Fig. 5, both the density and temperature profiles can be seen.

Since we now have a plasma-discharge where there is a strong reduction in the E×B-shear between two flattop time-intervals, we can examine how TGLF responds to that. Since in the simulations of our reference discharge #32305 there was a significant increase in the ion heat flux with decreasing E×B-shear, we can expect the ion temperature profile of the time-interval where NBI was replaced with ICRF to be flatter than the experimentally measured one.

As can be seen in Fig. 6 (a), to an extent this is indeed what happens. Using the same settings as the simulations done in section 2, we find that in the case where only NBI and ECRH are used for heating the plasma, the TGLF simulation results in a good match outside r/a= 0.25, and an under-prediction

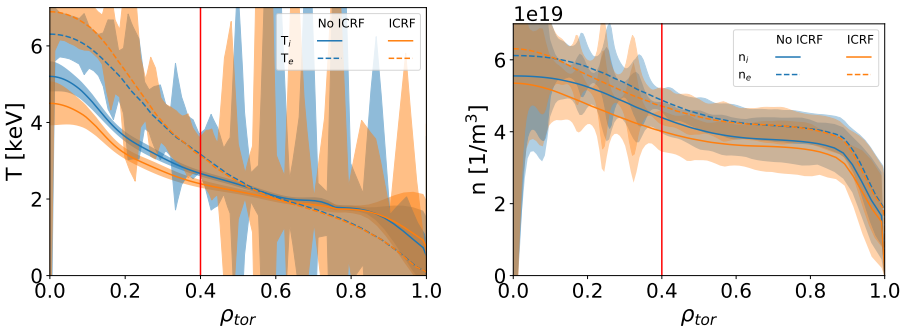

Figure 5: Radial profiles of the temperatures (a) and densities (b). Blue lines correspond to an average over the first time interval indicated in Fig. 3, orange lines to the average over the second one. Dashed lines correspond to electron temperatures and densities, while the unbroken lines correspond to the temperatures and densities of the ions. The shaded regions represent the sum of one standard deviation of that average and the propagated measurement uncertainties. The red lines indicate the radial position $\rho_{\mathrm{tor}} = 0.4$, at which position the time-traces in Fig. 3 were plotted.

of T_i in the very center, just like the simulations of #32305. As we expected, for the second time-interval with the reduced $E \times B$-shear, the ion temperature gradient is much flatter between r/a= 0.25 and r/a= 0.4.

To be able to compare the quality of different simulations with each other, we calculate the average normalized deviation from the experimental data

$$d = \frac{1}{N} \sum_{0.2<r/a<0.5} \frac{|T_{\mathrm{i,sim}} - T_{\mathrm{i,exp}}|}{T_{\mathrm{i,exp}}}, \tag{3}$$

where N is the number of points in the interval $0.2 < r/a < 0.5$. This interval was chosen because it is the approximate range in which the reduction of ITG turbulence is observed. For the shot #35938, in the time interval with reduced E×B-shear, we get a value of $d = 5.6\,\%$, which indicates a significantly poorer match than in the time interval without ICRF where $d = 2.9\,\%$.

Close to the boundary, at $r/a = 0.75$, we have observed TGLF to underestimate the heat flux, leading to higher gradients. This has been consistently observed also for other machines[18][19] and will be resolved in an upcoming revision of TGLF.

For the simulations presented in Fig. 6 (a), this was partially compensated by adding an additional artificial flux localized at the boundary, shifting the ion temperature profiles there down to the experimentally measured values. In the second time interval, however, outside r/a≈0.4 the simulated heat flux is still slightly underestimated.

A plasma discharge that is very similar to AUG #35938, in that some NBI

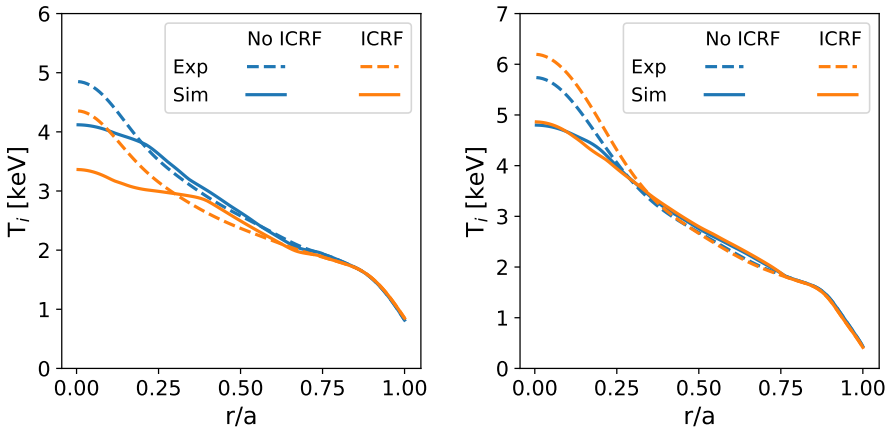

(a) (b)

Figure 6: Ion temperature profiles of the AUG shots #35938 (a) and #36072 (b) comparing the results of TGLF simulations (solid lines) to the experimental profiles (dashed lines), at a time interval without ICRF (blue) and with ICRF (orange). The setup is the same as for the simulations described in section 2, including both fast ion and $E \times B$ effects.

was replaced with ICRF to reduce the $E \times B$-shear, is the discharge AUG #36072. For this discharge, TGLF simulations do not display this problem of the underestimated heat fluxes. The difference between these two discharges is that different NBI sources were used and that in the second half of #36072 one of the off-axis NBI sources was lost, changing the equilibrium. As a result, there was only a small reduction in $\omega_{E\times B}$ observed, which is not significant compared to the uncertainties. As a result no experimental conclusions can be drawn from the unchanged ion temperature gradient. Consequently, TGLF simulations of this discharge (Fig. 6 (b)) show little change between the time interval with and without ICRF. In both cases, the measured peaked T_i could not reproduced by TGLF.

Nevertheless, in the TGLF simulations, this small change in $\omega_{E\times B}$ already leads to a much poorer match in the time interval with ICRF ($d = 4.6\,\%$) compared to the time interval without ICRF ($d = 2.2\,\%$).

4 New approach to simulations

In the previous sections, we established both experimentally and with simulations that in TGLF the effect of the $E \times B$-shear on the reduction of turbulent transport is strongly overestimated. In turn, other effects that are found to be the relevant contributors to the stabilisation of the ITG are strongly un-

derestimated, in particular the electromagnetic fast ion effect but also effects coming from the thermal pressure. In some cases, such as our reference discharge #32305, these two faults in the code can compensate. This, however, is of course not true for the general case, as was shown in section 3. If we want to continue modelling such non-inductive high-beta advanced scenarios using TGLF, we therefore need to somehow implement the missing effects into it. For this, an ad hoc model is proposed, that is explained in the following:

As a first step, we deactivate $\mathrm{E}\times\mathrm{B}$ effects, as they do not seem to play a role in our experiments. After that, we need to find a way to somehow stabilise the ITG-modes in a way that includes the combination of all effects affecting the ITG not yet or not properly implemented in TGLF. To do this, we use another stabilizing effect that is already implemented in TGLF, the dilution effect, to mimic the missing effects. This is done by adding an artificial second impurity to TGLF, the density of which is proportional to the cumulative strength of the missing effects. This way we can use the dilution of the main species to reduce the ion heat flux that TGLF gives as output. It is important to note here that this artificial impurity is only included in TGLF, not in ASTRA, and the only influence this impurity has is through its dilution effect affecting the deuterium energy flux. There is no heat flux attached directly to this impurity. Inside ASTRA everything remains unchanged, with the exception of the modified ion heat flux it gets from TGLF,to model the reduced transport correctly.

Finding a formula that works reliably over a larger range of scenarios and that can be scaled to other devices is still work to be done, but first preliminary results using the heuristic formula

$$n_{\mathrm{imp}} = k \cdot p_{\mathrm{fast}} \cdot e^{-\mathrm{s}} \tag{4}$$

already yield promising results, as can be seen in figures 7, 8 and 9. By including the fast ion pressure p_{fast}, fast ion effects are taken into account, and by including the magnetic shear s in the exponential function, we implement the observation that a reversed magnetic shear leads to a reduction of turbulent transport. Using this preliminary formula we also have to include a fit parameter k, which limits the predictive capabilities of this new method in its current form. As a next step it is intended to find a formula that more accurately describes the missing effects, which does not need such a fit factor anymore.

In Fig. 7, the ion temperature profiles from several TGLF simulations of the AUG discharge #32305 using the new method with different values of k are compared to the experimental profiles. It can be seen that the dependence of k is not that strong, with a change of approximately 50 % affecting the profiles only a little. Using this new method, it is possible to reproduce the peaking of the ion temperature quite well, with our quality factor $d = 1.8\,\%$ being fairly low with the right value of k.

For comparison, results are also shown of simulations of the two discharges in which some NBI is replaced with ICRF, using the new method.

In Figure 8, one can see results of the discharge where the $E \times B$-shear was successfully reduced (#35938). Like with the simulations using fast ion and

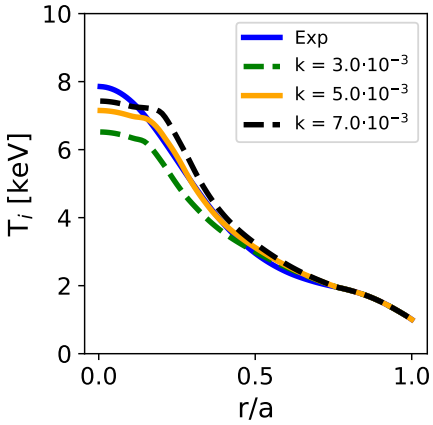

Figure 7: Ion temperature profiles resulting from TGLF simulations of the discharge #32305 using the new model, compared to the experimental profile. Depicted are the results using different values of the free parameter k.

$E \times B$-shear effects, in the case of the time interval without ICRF, the resulting profiles are a good match ($d = 0.4\,\%$), in the case of the time interval with ICRF, the ion temperature is again slightly overestimated towards the edge, resulting in a poor match ($d = 6.0\,\%$). This is despite having again added an additional ion heat flux at the boundary. In the case with additional ICRF we also find that if we increase k too much, the temperature profile collapses in the core. Still, it is possible for both time intervals to get reasonable results that are as good or better than the results obtained without this new method, using the same value of $k = 0.2 \times 10^{-3}$.

Looking at the results of simulations of the discharge in which it was not possible to significantly reduce the $E \times B$-shear (#36072) using the new method, shown in Fig. 9, we can nicely see that with this approach we can very well reproduce the experimental curves ($d = 1.2\,\%$ without ICRF and $d = 0.7\,\%$ with ICRF). Though in this case, the required fit-factor k varies by a factor of 3 between the two different time intervals, pointing to a need to modify and add additional parameter dependencies to the formula used.

In all the simulations using this new method, the artificial impurity added was Carbon-18, a non-existing species. The choice of mass and charge of this new species is such as to not overlap its resonances with neither deuterium nor boron. Within this constraint, any other choice of mass and charge would do. A variation of these two parameters does not alter the results, as long as the dilution obtained in the end is the same.

We want to stress that while this method is partially physics-based, it is still only a provisional workaround. In the long term, the electromagnetic fast ion effects need to be properly implemented in TGLF.

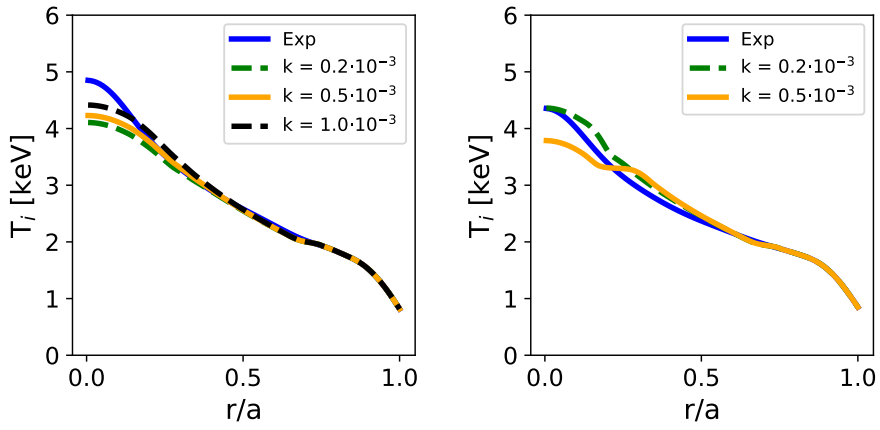

(a) (b)

Figure 8: Ion temperature profiles resulting from TGLF simulations of the AUG discharge #35938 using the new method, compared to the experimental profiles. Depicted are the results using different values of the free parameter k, of the time interval without ICRF (a) and with ICRF (b).

5 Summary and outlook

An experiment that aims to study the effect of the E×B-shear on the suppression of ITG turbulence has been conducted in the tokamak ASDEX Upgrade. This was done on an advanced scenario discharge where approximately 80% of the current were non-inductively driven, with $\beta_N \approx 2.6$, $H_{98}(y, 2) > 1$ and a plasma-current of 800 kA. In this experiment it was found that a reduction of the E×B-shear does not correspond to a change in R/L_{T_i}. To get a clearer picture, further experiments of this type, using different scenarios, are planned, though this finding is supported by simulations using the gyrokinetic code GENE, where changing the $E \times B$-shear did not affect the ion heat-flux.

Contrary to that, in simulations using the quasilinear transport model TGLF, the $E \times B$-shear has a big effect on the ion temperature profiles in such high beta scenarios, which in general leads to the model not being able to accurately reproduce the experimental results.

To be able to use TGLF despite this overestimation of the E×B-shear, we proposed an alternate ad hoc model that tries to mimic all the effects that are necessary to properly reproduce the experimentally found reduced ion heat flux in TGLF. This model is still under development, where additional experiments and simulations using GENE will serve as basis. Nevertheless, a preliminary formula already yielded promising results.

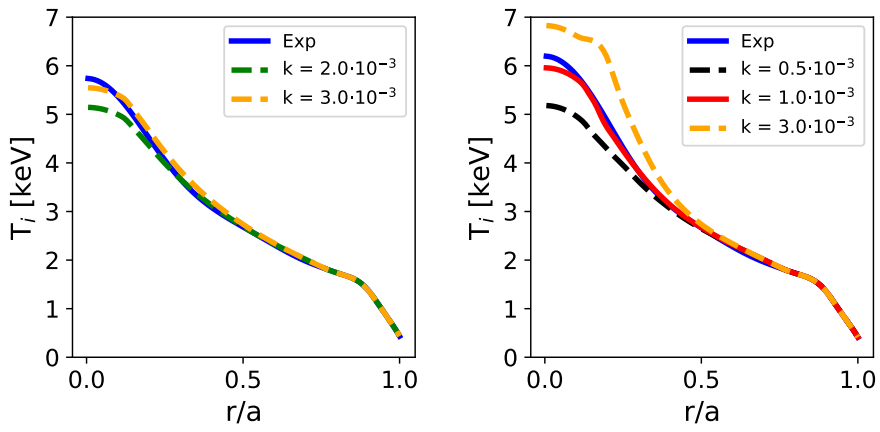

(a) (b)

Figure 9: Ion temperature profiles resulting from TGLF simulations of the AUG discharge #36072 using the new method, compared to the experimental profiles. Depicted are the results using different values of the free parameter k, of the time interval without ICRF (a) and with ICRF (b).

Acknowledgements

This work has been carried out within the framework of the EUROfusion Consortium and has received funding from the Euratom research and training programme 2014-2018 and 2019-2020 under grant agreement No 633053. The views and opinions expressed herein do not necessarily reflect those of the European Commission.

References

[1] A. Bock et al. Non-inductive improved h-mode operation at ASDEX upgrade. *Nuclear Fusion*, 57(12):126041, oct 2017.

[2] G. M. Staebler et al. A theory-based transport model with comprehensive physics. *Physics of Plasmas*, 14(5):055909, 2007.

[3] J.E. Kinsey et al. ITER predictions using the GYRO verified and experimentally validated trapped gyro-landau fluid transport model. *Nuclear Fusion*, 51(8):083001, jun 2011.

[4] Hyun-Tae Kim et al. Statistical validation of predictive TRANSP simulations of baseline discharges in preparation for extrapolation to JET D–T. *Nuclear Fusion*, 57(6):066032, may 2017.

[5] F. Sommer et al. Transport properties of h-mode plasmas with dominant electron heating in comparison to dominant ion heating at ASDEX upgrade. *Nuclear Fusion*, 55(3):033006, feb 2015.

[6] E. Fable et al. Selected transport studies of a tokamak-based DEMO fusion reactor. *Nuclear Fusion*, 57(2):022015, sep 2016.

[7] H. Doerk et al. Turbulence in high-beta ASDEX Upgrade advanced scenarios. *Nuclear Fusion*, 58(1):016044, dec 2017.

[8] A. Bock et al. Advanced tokamak investigations in full-tungsten ASDEX Upgrade. *Physics of Plasmas*, 25(5):056115, 2018.

[9] J. Citrin et al. Nonlinear stabilization of tokamak microturbulence by fast ions. *Phys. Rev. Lett.*, 111:155001, Oct 2013.

[10] A. Di Siena et al. Electromagnetic turbulence suppression by energetic particle driven modes. *Nuclear Fusion*, 59(12):124001, sep 2019.

[11] F. Jenko et al. Electron temperature gradient driven turbulence. *Physics of Plasmas*, 7(5):1904–1910, 2000.

[12] G.V. Pereverzev and P.N. Yushmanov. *ASTRA - Automated System for TRansport Analysis*, 2002.

[13] E Fable et al. Novel free-boundary equilibrium and transport solver with theory-based models and its validation against ASDEX Upgrade current ramp scenarios. *Plasma Physics and Controlled Fusion*, 55:124028, 12 2013.

[14] Xiang Jian et al. Key effects on the confinement improvement of the ASDEX upgrade hybrid scenario. *Nuclear Fusion*, 59(10):106038, sep 2019.

[15] G.M. Staebler et al. A new paradigm for ExB velocity shear suppression of gyro-kinetic turbulence and the momentum pinch. *Nuclear Fusion*, 53(11):113017, sep 2013.

[16] R. Fischer et al. Coupling of the flux diffusion equation with the equilibrium reconstruction at ASDEX Upgrade. *Fusion Science and Technology*, 69(2):526–536, 2016.

[17] R. Fischer. Estimation and uncertainties of profiles and equilibria for modelling codes. to be published.

[18] J. E. Kinsey et al. Predictions of the near edge transport shortfall in DIII-D L-mode plasmas using the trapped gyro-landau-fluid model. *Physics of Plasmas*, 22(1):012507, 2015.

[19] P Mantica et al. Progress and challenges in understanding core transport in tokamaks in support to ITER operations. *Plasma Physics and Controlled Fusion*, 62(1):014021, dec 2019.